High Temperatures-High Pressures, Vol. 41, pp. 81–97
Reprints available directly from the publisher
Photocopying permitted by license only

Equation of state for benzene for temperatures from the melting line up to 725 K with pressures up to 500 MPa†

MONIKA THOL,[1,2,*] ERIC W. LEMMON[2] AND ROLAND SPAN[1]

[1]*Thermodynamics, Ruhr-University Bochum,*
Universitaetsstrasse 150, 44801 Bochum, Germany
[2]*National Institute of Standards and Technology, 325 Broadway,*
Boulder, Colorado 80305, USA

Received: December 23, 2010. Accepted: April 17, 2011.

An equation of state (EOS) is presented for the thermodynamic properties of benzene that is valid from the triple point temperature (278.674 K) to 725 K with pressures up to 500 MPa. The equation is expressed in terms of the Helmholtz energy as a function of temperature and density. This formulation can be used for the calculation of all thermodynamic properties. Comparisons to experimental data are given to establish the accuracy of the EOS. The approximate uncertainties ($k = 2$) of properties calculated with the new equation are 0.1% below $T = 350$ K and 0.2% above $T = 350$ K for vapor pressure and liquid density, 1% for saturated vapor density, 0.1% for density up to $T = 350$ K and $p = 100$ MPa, 0.1 – 0.5% in density above $T = 350$ K, 1% for the isobaric and saturated heat capacities, and 0.5% in speed of sound. Deviations in the critical region are higher for all properties except vapor pressure.

Keywords: Benzene, equation of state, extrapolation behavior, Helmholtz energy, thermodynamic properties.

*Corresponding author: M.Thol@thermo.ruhr-uni-bochum.de

†Paper presented at the Ninth Asian Thermophysical Properties Conference, October 19-22, 2010, Beijing, China.

1 INTRODUCTION

1.1 Characteristics of Benzene

Benzene (C_6H_6) is included in the family of aromatic hydrocarbons. It is a colorless liquid at atmospheric conditions. It is flammable and potentially explosive when it is mixed with air in its gaseous form, and its vapors are toxic. Benzene is used as an additive to gasoline to increase the knock resistance. The chemical industry needs benzene for the synthesis of many products, e.g., polymers, nitrobenzene, aniline, phenol, insecticides, plastics, and synthetic resin. Furthermore, it is used in the fabrication of detergent and as a solvent for varnish, resin, waxes, and oils [1].

Due to these industrial uses, benzene has been widely measured to characterize its chemical, thermal, caloric, and combustion properties. In the thermodynamics area, experimental data are available for density, vapor pressure, speed of sound, virial coefficients, heat capacities, and enthalpy of vaporization. The physical characteristics and properties of benzene are given in Table 1.

1.2 Previous Equations of State

There are two equations of state available for benzene. The equation of Goodwin [4] is derived from phase boundaries like the melting line. It is written in an uncommon form, so it is difficult to implement into conventional software packages. Until today the most recent and commonly used equation of state for benzene is a Bender-type equation from 1992 developed by Polt *et al*. [3]. It is valid for a temperature range of $T = (283 - 635)\,\mathrm{K}$ and pressures up to $p = 78\,\mathrm{MPa}$. It was fitted to densities and saturation data (saturated liquid densities, saturated vapor densities and vapor pressures). Additional data and new fitting techniques are available now, so that other properties, e.g. heat capacities or speeds of sound, can also be used to fit an equation of state.

TABLE 1
Physical characteristics and properties of benzene.

Symbol	Property	Value
M	Molar mass [2]	$78.1118\ \mathrm{g{\cdot}mol^{-1}}$
T_c	Critical temperature [3]	562.02 K
p_c	Critical pressure	4.894 MPa
ρ_c	Critical density	$3.902\ \mathrm{mol{\cdot}dm^{-3}}$
T_{tp}	Triple point temperature	278.674 K
T_b	Reference temperature for ideal gas properties at the boiling point	353.21635 K
p_b	Reference pressure for ideal gas properties at the boiling point	0.101325 MPa

2 THE NEW EQUATION OF STATE

The new equation of state is written in terms of the reduced molar Helmholtz free energy as a function of temperature and density. The equation is composed of separate terms arising from ideal-gas behavior (superscript 0) and a "residual" or "real-fluid" (superscript r) contribution:

$$\alpha(\tau,\delta)=\frac{a^0(\rho,T)+a^{\mathrm{r}}(\rho,T)}{RT}=\alpha^0(\tau,\delta)+\alpha^{\mathrm{r}}(\tau,\delta), \tag{1}$$

where R is the molar gas constant.

The ideal-gas contribution is based on a $c_p{}^0$ equation represented as

$$\frac{c_p^0}{R}=3.94645+\sum_{k=3}^{5}v_k\frac{u_k^2\exp(u_k)}{\left[\exp(u_k)-1\right]^2} \tag{2}$$

with $v_3=7.36374$, $v_4=18.649$, $v_5=4.01834$, $u_3=4116$ K/T, $u_4=1511$ K/T, $u_5=630$ K/T, and $R=8.314472$ J·mol^{-1}K^{-1}. The parameters of the $c_p{}^0$ equation were fitted to experimental values of the ideal-gas heat capacity of Burcat *et al.* [5] and evaluated values from the Thermo Data Engine (TDE) [6] of the National Institute of Standards and Technology.

The $c_p{}^0$ equation has to be integrated so that the ideal-gas contribution α^0 can be given as

$$\alpha^0=\ln(\delta)+2.94645\ln(\tau)+a_1+a_2\tau+\sum_{k=3}^{5}v_k\ln\left(1-\exp\left[-b_k\tau\right]\right), \tag{3}$$

where $a_1=-0.6740687105$, $a_2=2.5560188958$, $b_3=7.323583$, $b_4=2.688516$, $b_5=1.1209566$, and the values of v_k are the same as those in Eq. (2). The values for a_1 and a_2 are calculated so that $h=0$ kJ·kg^{-1} and $s=0$ kJ·kg^{-1}K^{-1} at the normal boiling point for the liquid state.

Comparisons of experimental and theoretical ideal, isobaric heat capacities with calculated values from the equation of state are shown in Figure 1.

The real-fluid contribution is given by

$$\begin{aligned}\alpha^{\mathrm{r}}=&\sum_{i=1}^{5}n_i\delta^{d_i}\tau^{t_i}+\sum_{i=6}^{10}n_i\delta^{d_i}\tau^{t_i}\exp\left[-\delta^{p_i}\right]\\&+\sum_{i=11}^{14}n_i\delta^{d_i}\tau^{t_i}\exp\left(-\eta_i(\delta-\varepsilon_i)^2-\beta_i(\tau-\gamma_i)^2\right),\end{aligned} \tag{4}$$

where the temperature and density are expressed in the dimensionless variables $\tau=T_c/T$ and $\delta=\rho/\rho_c$. The critical temperature $T_c=(562.02\pm0.15)$ K of Polt *et al.* [3] was adopted. The critical density $\rho_c=(3.902\pm0.05)$ mol·dm^{-3} was fitted in this work. The critical pressure $p_c=(4.894\pm0.015)$ MPa was cal-

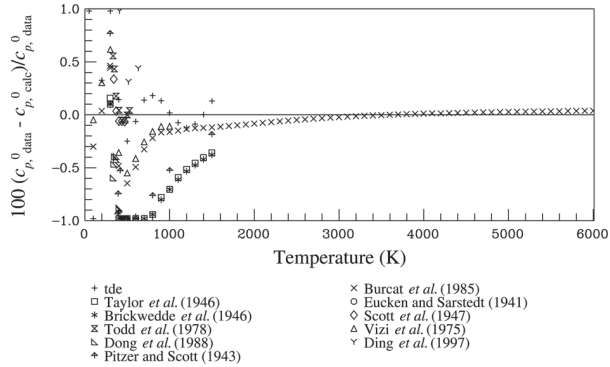

FIGURE 1
Comparisons of ideal gas heat capacities c_p^0 calculated with the equation of state to experimental and theoretical data as a function of temperature T.

culated from the new equation of state. The n_i are numerical coefficients fitted to experimental data. The first and second summations represent the more common form of the equation of state. The third summation improves the representation of the properties in the critical region; these terms go to zero far away from the critical point. The parameters for Eq. (4) are given in Table 2. The equation of state was fitted to experimental data by use of nonlinear fitting methods. In addition to optimizing the parameters to the data, numerous thermodynamic constraints were applied to ensure that the equation was well behaved and would reliably extrapolate beyond the range of the available data. These techniques enable a comprehensive equation of state with a relatively small number of terms. Nonlinear fitting requires starting values for all of the parameters and exponents, and an unpublished 14-term equation for propane was used as the starting point. The Helmholtz energy equation of state and the fitting process is described in detail by Lemmon *et al.* [7]; that paper also describes the calculation of all the thermodynamic properties from the Helmholtz energy.

3 EXPERIMENTAL DATA AND COMPARISONS TO THE EQUATION OF STATE

Since the identification of benzene in 1825 by Michael Faraday, many experimental studies of the thermodynamic properties of benzene have been reported. Selected data were used for the development of the new thermodynamic property formulation reported here. Comparisons were made to all available experimental data, including those not used in the development of the equation of state. Because of the large data sets, the figures presented in this work only include data that are located within the given accuracy range

TABLE 2
Coefficients, temperature and density exponents and Gaussian bell-shaped parameters for the residual Helmholtz energy α^r in Eq. (4).

i	n_i	t_i	d_i	p_i	η_i	β_i	γ_i	ε_i
1	0.03513062	1	4					
2	2.229707	0.3	1					
3	–3.100459	0.744	1					
4	–0.5763224	1.174	2					
5	0.2504179	0.68	3					
6	–0.7049091	2.5	1	2				
7	–0.1393433	3.67	3	2				
8	0.8319673	1.26	2	1				
9	–0.3310741	2.6	2	2				
10	–0.02793578	0.95	7	1				
11	0.7087408	1	1		1.032	1.867	1.118	0.7289
12	–0.3723906	2.47	1		1.423	1.766	0.6392	0.9074
13	–0.06267414	3.35	3		1.071	1.824	0.6536	0.7655
14	–0.86295	0.75	3		14.35	297.5	1.164	0.8711

of the equation unless no more reliable data are available. For comparisons with every available data set see [8].

The accuracy of the equation of state was determined by statistical comparisons of calculated property values to experimental data. These statistics are based on the percent deviation in any property X, defined as

$$\Delta X = 100\left(\frac{x_{\text{data}} - x_{\text{calc}}}{x_{\text{data}}}\right). \tag{5}$$

With this definition, the average absolute relative deviation is defined as

$$\text{AAD} = \frac{1}{n}\sum_{i=1}^{n}\left|\Delta X_i\right|, \tag{6}$$

where n is the number of data points.

3.1 Comparisons with Saturation Thermal Data

In Figure 2 comparisons of vapor pressures calculated from the equation of state with experimental data are shown. As this paper was a conference contribution it is limited in size. For the references for each data point see [8]. There are many data up to $T = 350\,\text{K}$ and the deviations of most of the data

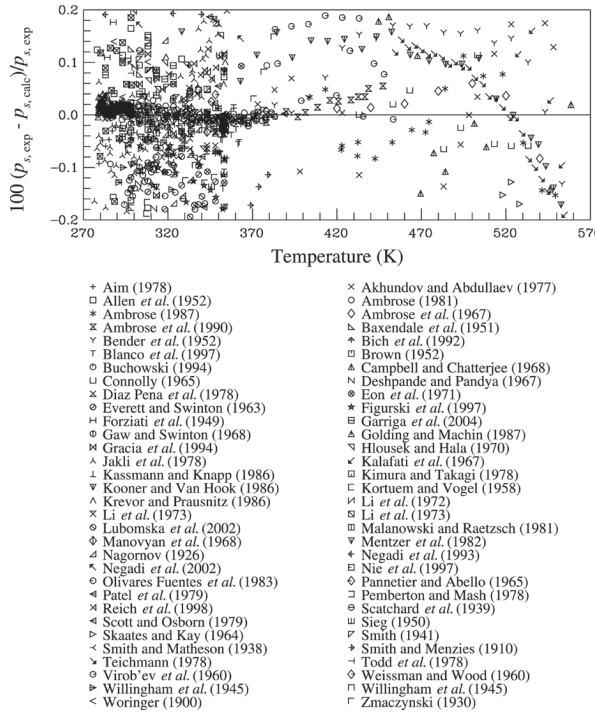

FIGURE 2
Comparisons of vapor pressure p_s calculated with the equation of state to experimental data as a function of temperature T.

are within 0.1%. The new equation of state conforms well to the data set of Ambrose [9] (AAD = 0.017%). Above this temperature there is just a small number of data points and the deviations increase to 0.2%, but with still a few high-accuracy data sets, e.g., Ambrose *et al.* [10] (AAD = 0.014%).

Comparisons of saturated liquid densities calculated from the equation of state with experimental data are presented in Figure 3. There are many values of liquid density up to $T = 350$ K that scatter around the equation within less than 0.1%. The data set of Sun *et al.* [11] (AAD = 0.054%) is represented very well. Above $T = 350$ K there are only seven data sets. The expected uncertainty of the equation is 0.2%. The equation agrees very well with the data measured by Hales and Townsend [12] (AAD = 0.024%) and Chirico ad Steele [13] (AAD = 0.043%).

A comparison of saturated vapor densities calculated from the equation of state with experimental data is depicted in Figure 4. There is no recent data set available for the saturated vapor densities, so it is not possible to achieve a smaller uncertainty of the equation than 1%. The data, which are reflected best by the equation, are measured by Akhundov and Abdullaev [14] (AAD = 0.508%).

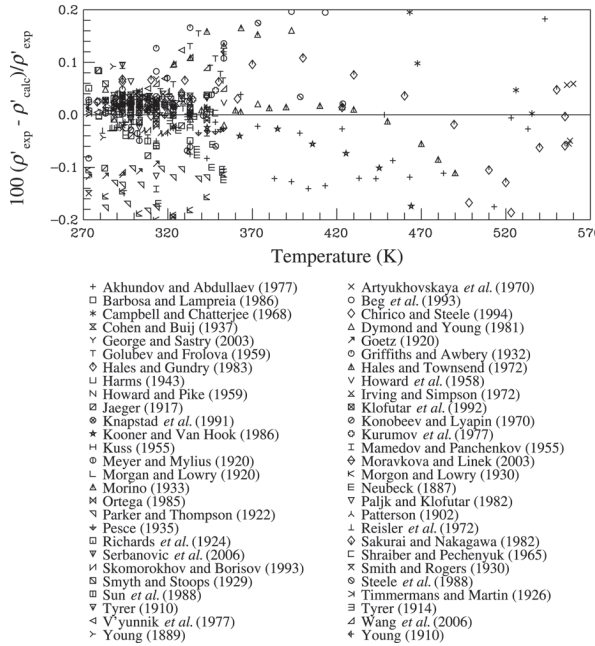

FIGURE 3
Comparisons of saturated liquid densities ρ' calculated with the equation of state to experimental data as a function of temperature T.

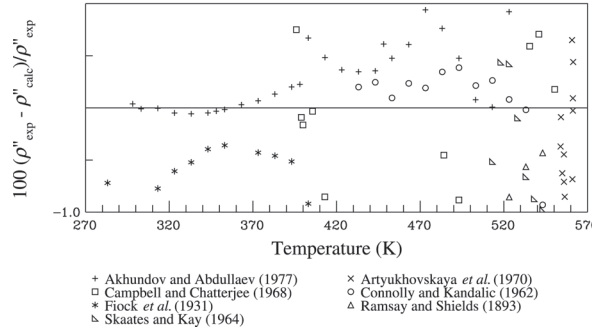

FIGURE 4
Comparisons of saturated vapor densities ρ'' calculated with the equation of state to experimental data as a function of temperature T.

3.2 $p\rho T$ Data and Virial Coefficients

An overview of the deviations of experimental densities and densities calculated with the new equation of state is given in Figure 5. For clarity, in the extended critical region pressure deviations are also shown in Figure 6. The

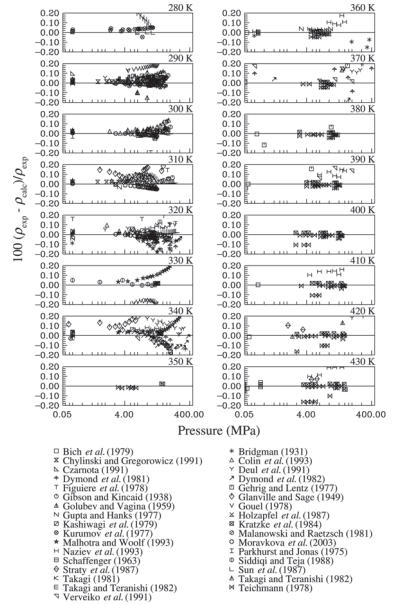

FIGURE 5
Comparisons of densities ρ calculated with the equation of state to experimental data as a function of pressure p.

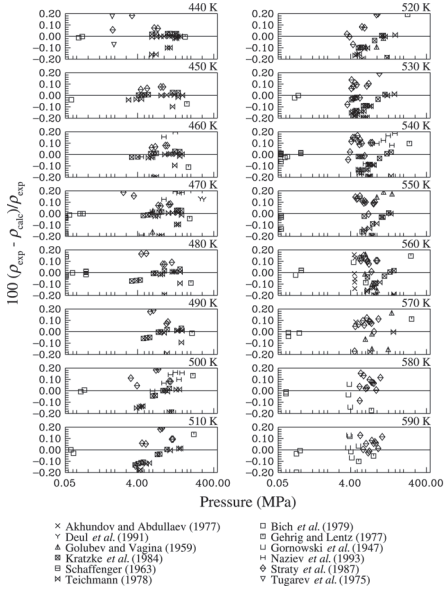

FIGURE 5. continued.

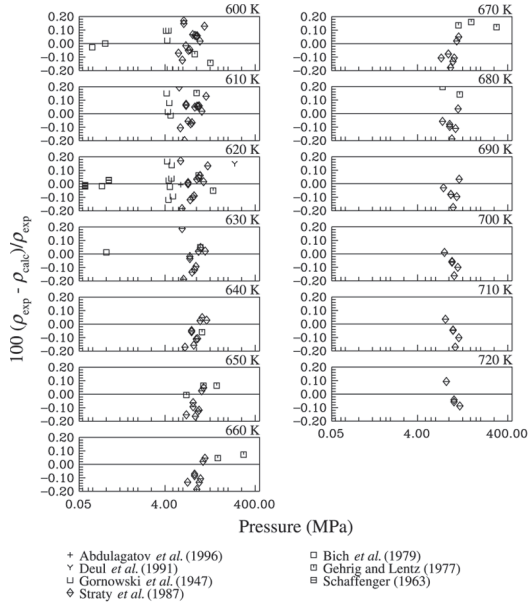

FIGURE 5. continued.

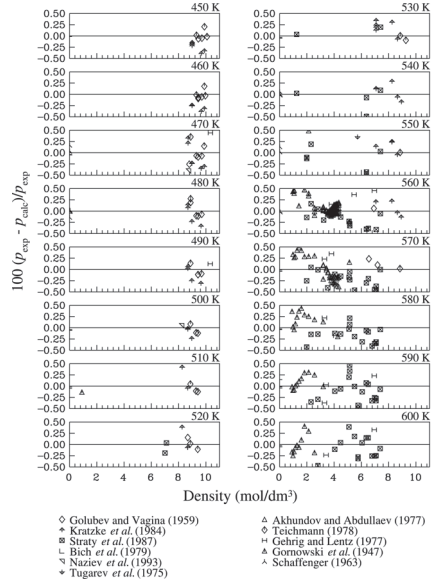

FIGURE 6
Comparisons of pressures p calculated with the equation of state to experimental data in the extended critical region as a function of density ρ.

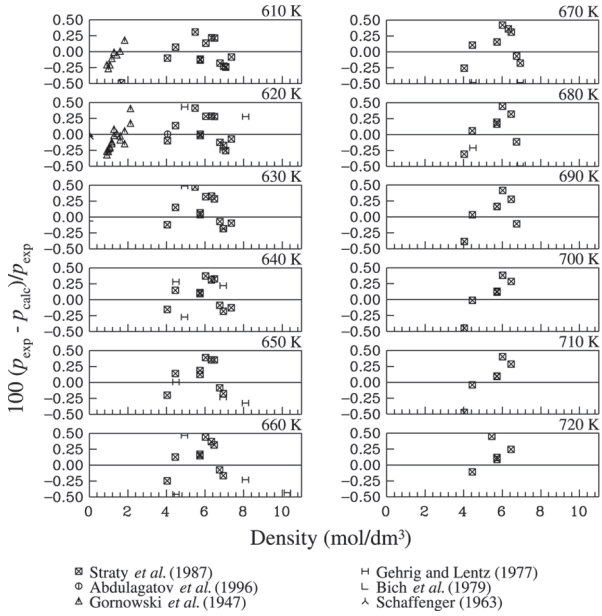

FIGURE 6. continued.

uncertainties for densities up to $T = 350\,\mathrm{K}$, and $p = 100\,\mathrm{MPa}$ are 0.1%. In this range the densities of Colin *et al.* [14] (AAD = 0.04%) and Moravkova *et al.* [15] (AAD = 0.022%) can be reproduced very well. Above $T = 350\,\mathrm{K}$ the deviations increase up to 0.1 – 0.5%. This region is presented well by Kratzke *et al.* [16] (AAD = 0.024%).

Figure 7 demonstrates the behavior of the second and third virial coefficients as well as the shape of the equation of state in the two-phase region. The lines show isotherms calculated from the equation of state, and the curve represents the saturated vapor density. The y-intercept ($\rho = 0$) represents the second virial coefficients at each given temperature, and the third virial coefficients are the slope of each line at zero density. Many equations of state show curvature in the lines at low temperatures caused by high values of the exponent t on temperature. As shown in this plot, there is no curvature in the lines, and the equation is extremely smooth and linear at low densities, as it should be (Lemmon and Jacobsen [18]).

3.3 Caloric Data

Figure 8 compares experimental enthalpies of vaporization to the equation of state. There have been no new measurements on the enthalpy of vaporization of benzene over the last 20 years, and many of the data available are generally fitted within 1%.

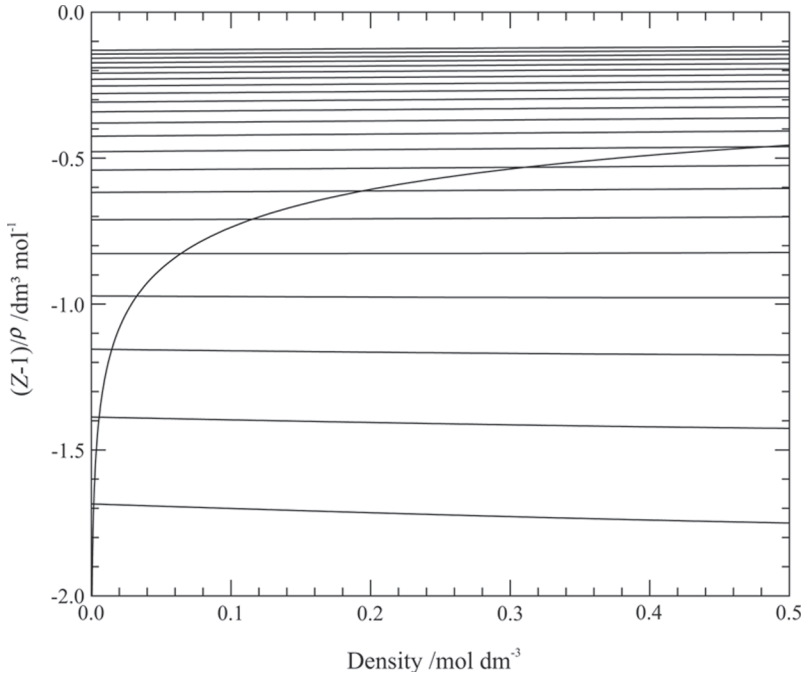

FIGURE 7
Calculations of $(Z - 1)/\rho$ along isotherms versus density ρ in the vapor phase.

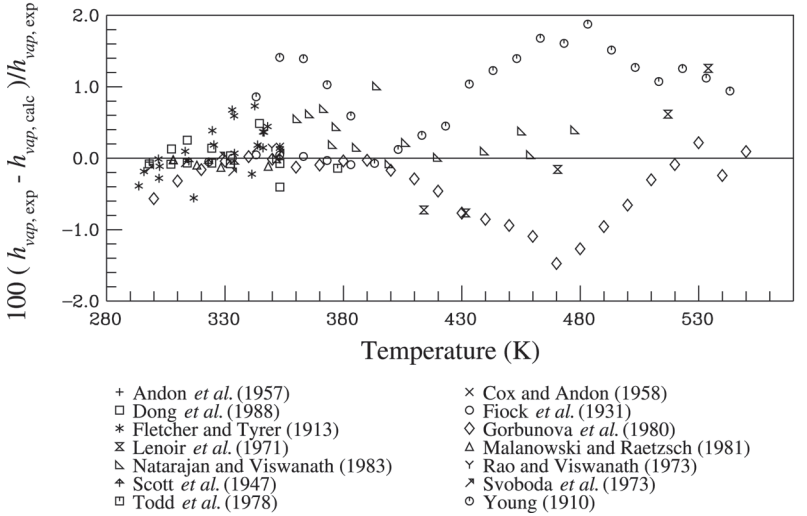

FIGURE 8
Comparisons of enthalpies of vaporization h_{vap} calculated with the equation of state to experimental data as a function of temperature T.

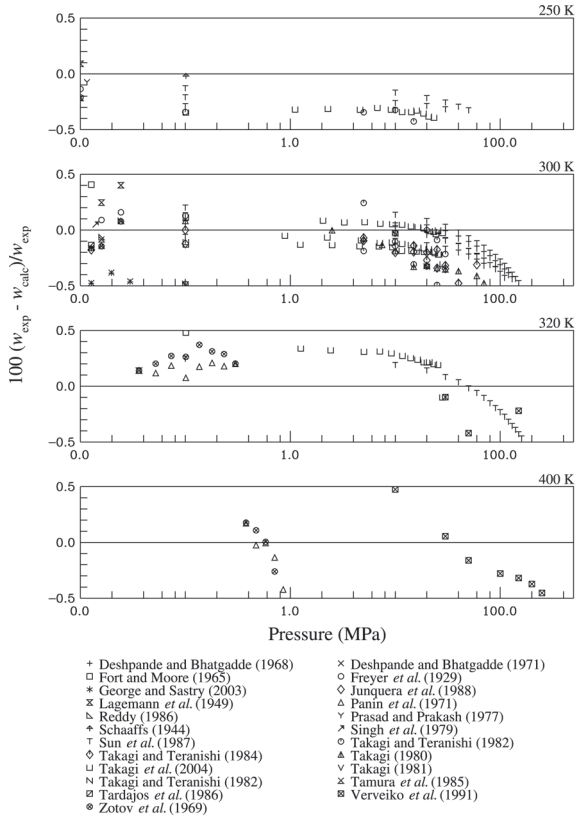

FIGURE 9
Comparisons of speed of sound w calculated with the equation of state to experimental data as a function of pressure p.

Most of the data for the speed of sound are in a small temperature range (T = 283 K – 333 K). There are just three authors who measured data at higher temperatures up to $T = 500$ K. Comparisons of values calculated from the equation of state for the speed of sound and high-accuracy experimental data are illustrated in Figure 9. It includes both saturated and homogenous data. The expected uncertainty of the equation is 0.5%. The saturated liquid speeds of sound were measured by Zotov *et al.* [19] (AAD = 0.36%) and Panin *et al.* [20] (AAD = 0.328%). The homogenous data of Takagi *et al.* [21] (AAD = 0.111%) and Takagi and Teranishi [22] (AAD = 0.176%) can be reproduced best.

In Figure 10 comparisons of experimental isobaric heat capacities and values calculated from the equation of state are shown. Figure 10 includes both saturated and homogenous data. The saturated liquid heat capacities that fit very well to the equation were measured by Nikolaev and Rabinovich [23] (AAD = 0.334%). In the homogenous region there are data from Todd *et al.* [24]

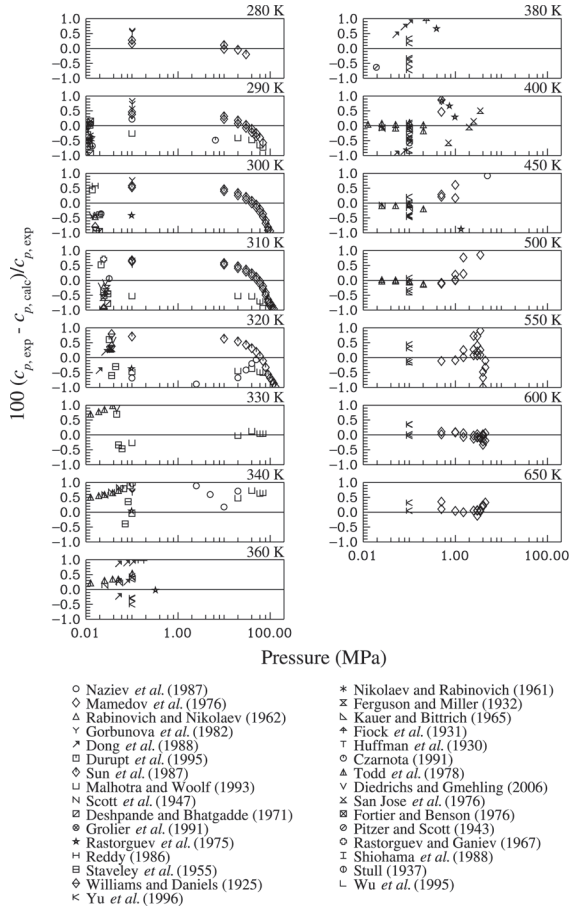

FIGURE 10
Comparisons of isobaric heat capacities c_p calculated with the equation of state to experimental data as a function of pressure p.

(AAD = 0.08%) and Yu *et al.* [25] (AAD = 0.288%), which conform best to the equation of state.

3.4 Extrapolation Behavior

The equation of state is valid from the triple point up to $T = 725$ K with pressures up to $p = 500$ MPa. For some applications it may be necessary to use the equation beyond these limitations. The extrapolation behavior of the thermodynamic properties is well-known (Lemmon and Jacobsen [18]). In the p versus ρ diagram the isotherms should converge, but not cross each other at high temperatures, pressures, and densities (Figure 11). Furthermore, the speed of

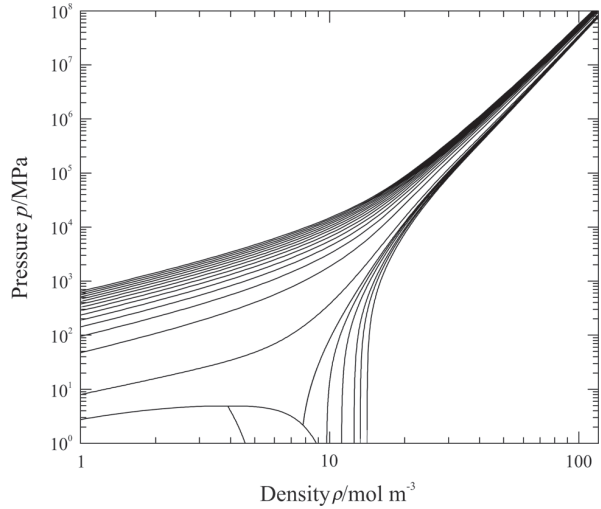

FIGURE 11
Isothermal behavior of the benzene equation of state at extreme conditions of temperature T and pressure p.

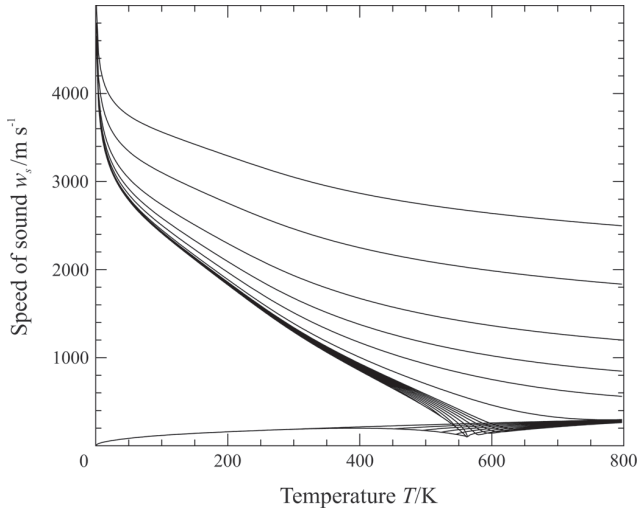

FIGURE 12
Speed of sound w versus temperature T diagram.

sound along the saturation lines and along isobars is shown in Figure 12. This plot shows reasonable behavior, especially since the saturation line for the liquid remains straight down to about $T = 50\,\mathrm{K}$, a reduced temperature of 0.08. The saturated vapor phase of the isobaric heat capacity should be straight

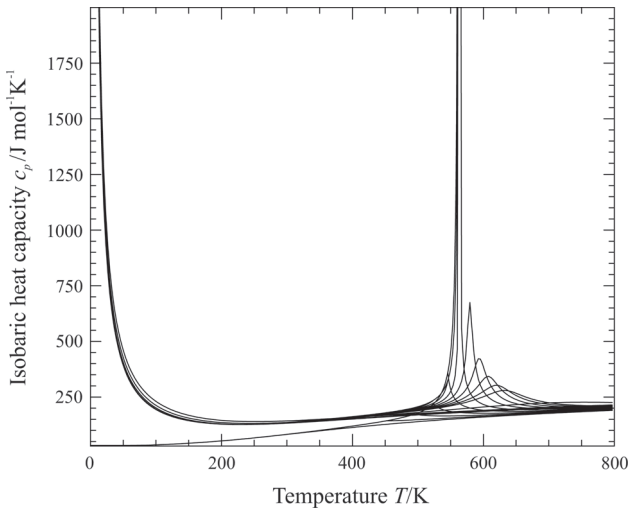

FIGURE 13
Isobaric heat capacity c_p versus temperature T diagram.

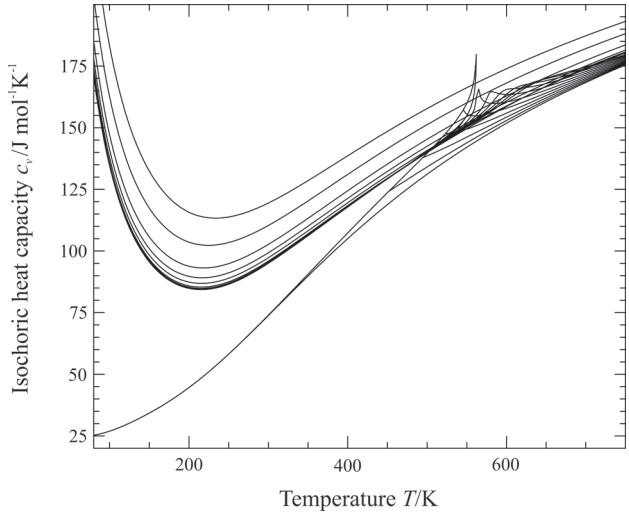

FIGURE 14
Isochoric heat capacity c_v versus temperature T diagram.

down to low temperatures. The hypothetically saturated liquid phase should rise approaching 0 K (Figure 13). The values of c_v should have a minimum in the liquid phase about half way down the saturation line (Figure 14). Finally the characteristic ideal curves of the equation of state for benzene should be smooth without any bumps as shown in Figure 15.

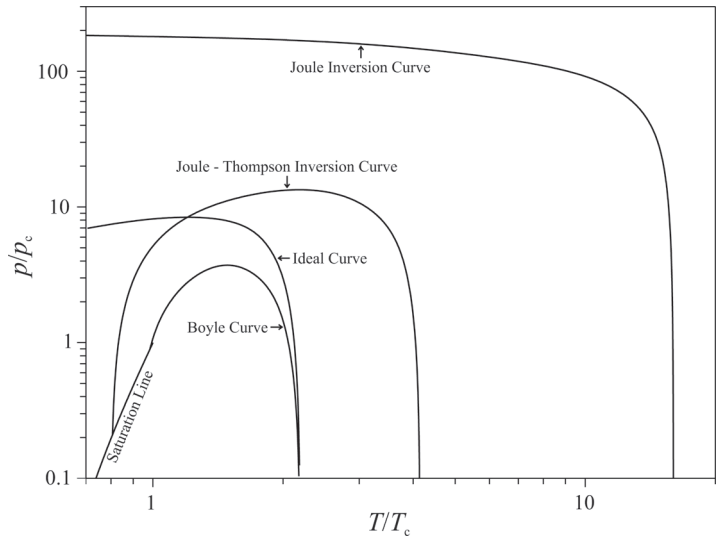

FIGURE 15
Characteristic (ideal) curves of the equation of state for benzene as a function of reduced temperature T/T_c and reduced pressure p/p_c.

4 CONCLUSION

In this work a new equation of state for benzene was developed, which consists of 14 terms (5 polynomial terms, 5 exponential terms and 4 Gaussian bell-shaped terms). As the equation is expressed in terms of the Helmholtz energy, it can be implemented easily in common software packages and used to calculate all thermodynamic properties, e.g., density, saturation state, heat capacity, speed of sound, and energy. The equation is valid from the triple point up to $T = 725\,\mathrm{K}$ with pressures up to $p = 500\,\mathrm{MPa}$. The extrapolation behavior is reasonable. With the help of large data sets the expected uncertainties are analyzed. The approximate uncertainties of properties calculated with the new equation are 0.1% below $T = 350\,\mathrm{K}$, and 0.2% above $T = 350\,\mathrm{K}$ for vapor pressure and liquid density, 1% for saturated vapor density, 0.1% for densities up to $T = 350\,\mathrm{K}$ and $p = 100\,\mathrm{MPa}$, 0.1 – 0.5% in density above $T = 350\,\mathrm{K}$, 1% for the isobaric heat capacity and saturated heat capacity, and 0.5% for speed of sound. Deviations in the critical region are higher for all properties except vapor pressures.

Please note: As this paper was a conference contribution it is limited in size. For more detailed information, see the publication in the Journal of Chemical Engineering Data [8].

NOMENCLATURE

Latin Symbols

Symbol	*Definition*	*Unit*
a	coefficients of the EOS for the ideal Helmholtz energy	–
AAD	average absolute relative deviation	–
c	heat capacity	$J \cdot mol^{-1}K^{-1}$
d	density exponents of the EOS for the residual Helmholtz energy	–
h	molar energy	$J \cdot mol^{-1}$
I	number of terms	–
M	molar mass	$g \cdot mol^{-1}$
n	coefficient of the EOS for the residual Helmholtz energy,	–
	number of data points	–
p	pressure,	MPa
	density exponents of the exponential part of the EOS for the residual Helmholtz energy	–
t	temperature exponents of the EOS for the residual Helmholtz energy	–
T	temperature	K
w	speed of sound	$m \cdot s^{-1}$
x	any thermodynamic property	–
Z	compressibility factor	–

Greek Symbols

Symbol	*Definition*	*Unit*
α	reduced Helmholtz energy	–
β	Gaussian bell-shaped parameter	–
γ	Gaussian bell-shaped parameter	–
δ	reduced density	–
ε	Gaussian bell-shaped parameter	–
η	Gaussian bell-shaped parameter	–
ρ	density	$mol \cdot dm^{-3}$
τ	reciprocal reduced temperature	–

Subscript

Symbol	*Definition*
calc	calculated by the EOS
exp	experimental
GB	Gaussian bell-shaped
p	isobaric

pol	polynomial
s	saturation
v	isochoric
vap	vaporization

Superscript

Symbol	*Definition*
'	saturated liquid
"	saturated vapor
0	ideal
r	residual

REFERENCES

[1] Deutsche Gesellschaft für Arbeitsmedizin und Umweltmedizin e. V. (German Society for Industrial and Environmental Medicine), Leitlinien, Universitaetsklinikum Schleswig-Holstein, Germany.
[2] Wieser M. E., Pure Appl. Chem., 78 (2006) 2051.
[3] Polt A., Platzer B., Maurer G. Chem. Tech. (Leipzig). 44 (1992) 216.
[4] Goodwin R. D., J. Phys. Chem. Ref. Data, 17 (1988) 1541.
[5] Burcat A., Zeleznik F. J., McBride B. J. NASA Tech. Memo X. (1985) 1.
[6] Frenkel M., Chirico R. D., Diky V., Muzny C. D., Kazakov A. F., Lemmon E. W. National Institute of Standards and Technology, Standard Reference Data Program: Gaithersburg, 2008.
[7] Lemmon E. W., Wagner W., McLinden M. O. Chem. Eng. Data. 54 (2009) 3141.
[8] Thol M., Lemmon E. W., Span R. J. Chem. Eng. Data. (2011), to be submitted.
[9] Ambrose D. J. Chem. Thermodyn. 13 (1981) 1161.
[10] Ambrose D., Ewing M. B., Ghiassee N. B., Sanchez Ochoa J. C. J. Chem. Thermodyn. 22 (1990) 589.
[11] Sun T. F., Schouten J. A., Trappeniers N. J., Biswas S. N. J. Chem. Thermodyn. 20 (1988) 1089.
[12] Hales J. L., Townsend R. J. Chem. Thermodyn. 4 (1972) 763.
[13] Chirico R. D., Steele W. V. Ind. Eng. Chem. Res. 33 (1994) 157.
[14] Akhundov T. S., Abdullaev F. G. Izv. Vyssh. Uchebn. Zaved, Neft Gaz. 20 (1977) 73.
[15] Colin A. C, Cancho S., Rubio R. G., Compostizo A. J. Phys. Chem. 97 (1993) 10796.
[16] Moravkova L., Wagner Z., Linek J. Fluid Phase Equilib. 209 (2003) 81.
[17] Kratzke H., Niepmann R., Spillner E., Kohler F. Fluid Phase Equilib. 16 (1984) 287.
[18] Lemmon E. W., Jacobsen R. T. J. Phys. Chem. Ref. Data. 34 (2005) 69.
[19] Zotov V. V., Neruchev Y. A., Otpushchennikov N. F. Russ. J. Phys. Chem. (Engl. Transl.) 43 (1969) 431.
[20] Panin P. P., Otpushchennikov N. F., Pankevich G. M. Uc. Zap. -Kursk. Gos. Ped. Inst. 91 (1971) 124.
[21] Takagi T., Sawada K., Urakawa H., Ueda M., Cibulka I. J. Chem. Thermodyn. 36 (2004) 659.
[22] Takagi T., Teranishi H. J. Chem. Thermodyn. 14 (1982) 1167.
[23] Nikolaev P. N., Rabinovich I. B. Tr. Khim. Khim. Tekhnol. (Gorki). 4 (1961) 242.
[24] Todd S. S., Hossenlopp I. A., Scott D. W. J. Chem. Thermodyn. 10 (1978) 641.
[25] Yu Q., Fang W., Zong H., Lin R. Thermochimica Acta. 275 (1996) 173.